AIP Applied Physics Letters

High operating temperature interband cascade focal plane arrays

Z.-B. Tian, S. E. Godoy, H. S. Kim, T. Schuler-Sandy, J. A. Montoya, and S. Krishna

Citation: Applied Physics Letters **105**, 051109 (2014); doi: 10.1063/1.4892634
View online: http://dx.doi.org/10.1063/1.4892634
View Table of Contents: http://scitation.aip.org/content/aip/journal/apl/105/5?ver=pdfcov
Published by the AIP Publishing

Articles you may be interested in
High operating temperature midwave infrared photodiodes and focal plane arrays based on type-II InAs/GaSb superlattices
Appl. Phys. Lett. **98**, 143501 (2011); 10.1063/1.3573867

High performance long wavelength infrared mega-pixel focal plane array based on type-II superlattices
Appl. Phys. Lett. **97**, 193505 (2010); 10.1063/1.3514244

High operating temperature 320 × 256 middle-wavelength infrared focal plane array imaging based on an In As In Ga As In Al As In P quantum dot infrared photodetector
Appl. Phys. Lett. **90**, 201109 (2007); 10.1063/1.2740111

Expandable fully reflective focal-plane optics for millimeter- and submillimeter-wave array receivers
Rev. Sci. Instrum. **77**, 014702 (2006); 10.1063/1.2165547

Two-dimensional micromechanical bimorph arrays for detection of thermal radiation
Appl. Phys. Lett. **70**, 3311 (1997); 10.1063/1.119147

AIP Journal of Applied Physics

Journal of Applied Physics is pleased to announce André Anders as its new Editor-in-Chief

This article is copyrighted as indicated in the article. Reuse of AIP content is subject to the terms at: http://scitation.aip.org/termsconditions. Downloaded to IP: 68.35.133.217 On: Thu, 07 Aug 2014 16:31:46

APPLIED PHYSICS LETTERS **105**, 051109 (2014)

High operating temperature interband cascade focal plane arrays

Z.-B. Tian, S. E. Godoy, H. S. Kim,[a] T. Schuler-Sandy, J. A. Montoya, and S. Krishna
Center for High Technology Materials, Department of Electrical and Computer Engineering, University of New Mexico, Albuquerque, New Mexico 87106, USA

(Received 29 May 2014; accepted 28 July 2014; published online 7 August 2014)

In this paper, we report the initial demonstration of mid-infrared interband cascade (IC) photodetector focal plane arrays with multiple-stage/junction design. The merits of IC photodetectors include low noise and efficient photocarrier extraction, even for zero-bias operation. By adopting enhanced electron barrier design and a total absorber thickness of 0.7 μm, the 5-stage IC detectors show very low dark current (1.10×10^{-7} A/cm^2 at -5 mV and 150 K). Even with un-optimized fabrication and standard commercial (mis-matched) read-out circuit technology, infrared images are obtained by the 320×256 IC focal plane array up to 180 K with *f*/2.3 optics. The minimum noise equivalent temperature difference of 28 mK is obtained at 120 K. These initial results indicate great potential of IC photodetectors, particularly for high operating temperature applications.
© *2014 AIP Publishing LLC*. [http://dx.doi.org/10.1063/1.4892634]

As a viable alternative to HgCdTe technology, antimony-based type-II superlattices (T2-SL) for high performance infrared (IR) detection have received much research interest.[1–5] Over the past decades, much progress has been made in both scientific and technological aspects with this material system.[1–5] Despite the relatively short carrier lifetime in InAs/Ga(In)Sb T2-SL, researchers have managed to take advantage of the great versatility in energy band engineering, and the performance of T2-SL detectors is steadily approaching that of the well-investigated HgCdTe and InSb technologies.[1–5] Medium-to-large format T2-SL based IR focal plane arrays (FPAs) with high operabilities have been reported,[2–4] with a noise equivalent temperature difference (NEDT) as low as 10 mK in mid-wave IR (MWIR),[2,3] and ~20 mK in long-wavelength IR (LWIR)[4] at 77 K.

Driven by the increasing demand for reduced size, weight, and power consumption (SWaP), the development of high operating temperature (HOT) IR FPAs are of great emphasis. The performance of IR detectors is ultimately determined by the signal to noise ratio (SNR). At higher operation temperatures, the increased thermal generation and scattering rates will generally degrade both the electrical and optical performances of T2-SL photodetectors. Therefore, maintaining a reasonably high response (efficient photocarrier extraction) with low noise at HOTs is the primary research focus. For conventional IR photodetectors, the photo-carrier extraction process is dominated by the drift-diffusion process, which is highly dependent on the electric field distribution and carrier lifetime. Generally, the electric field distribution in a photodetector is determined by the device structure and operation bias. An increased bias could promote photo-carrier extraction, but will also introduce much unwanted shot noise, thereby reducing the attainable SNR. In MWIR InAs/GaSb T2-SL materials, the Shockley-Read-Hall (SRH) lifetime will decrease to a few tens of nanoseconds at higher operating temperatures, which will drastically increase thermal noise and affect the photocarrier extraction. This makes it very challenging to obtain HOT operation for T2-SL.

One way to overcome these issues in T2-SL detectors is to use an interband cascade photodetector architecture.[5–7] Similar to the multi-junction designs,[8] which are widely adopted in high-efficiency photovoltaic solar cells, the IC structure is comprised of multiple stages electrically connected in series. Each stage contains a moderately thin absorber, which can be customized based on the particular applications. This allows the absorber to be split into relatively thin segments, for efficient photo-generated carrier collection. Unipolar barriers, which block the majority carriers without blocking the photo-generated carrier transport, are placed at each side of the thin absorbers. Due to the much shorter transport distance, the photo-carriers generated in these thin absorbers can be efficiently collected, even at very high operating temperatures where the diffusion length is greatly reduced. Furthermore, an ultra-fast (*sub-ps*) photo-generated carrier extraction channel–longitudinal optical (LO) photon assisted inter-subband relaxation, is utilized to provide very efficient photo-carrier transport. This is achieved by carefully constructing an electron stair-case energy ladder in the conduction band of electron relaxation regions. The device operation is shown in the schematic drawing of an IC detector in Fig. 1.

Unlike conventional multi-junction devices, where carrier transport between junctions/stages is realized by interband tunneling in highly doped P-N junctions, IC detectors fully take advantage of the inherent type-II broken-gap alignment in "6.1-Å-family" material system. In IC detectors, each cascade stage is composed of three regions. The first region is a finite InAs/GaSb T2-SL absorber region in which photo-excited carriers are generated; the second region is an electron relaxation (eR) region, which allows the photo-generated electrons to efficiently pass through; and the third region is an electron tunneling (eT) region which presents an electron barrier (eB) in the conduction band and meanwhile enables electrons to tunnel into the valence band of the next

[a]Current address: Department of Physics, Chonnam National University, Gwangju, 500-757, Republic of Korea.

 © 2014 AIP Publishing LLC

This article is copyrighted as indicated in the article. Reuse of AIP content is subject to the terms at: http://scitation.aip.org/termsconditions. Downloaded to IP: 68.35.133.217 On: Thu, 07 Aug 2014 16:31:46

stage.[5] The eR region is composed of carefully engineered coupled multiple-quantum-wells (MQWs) that form a series of stair-case energy ladders in the conduction band, with the energy separations close to an LO phonon energy. As mentioned earlier, a type-II broken-gap band alignment, between the eR region (in this stage) and the eT region (in the next stage) is adopted. This type-II broken-gap design facilitates a fast carrier relaxation path for photo generated electrons, leading to the very efficient collection of photo-generated carriers.[5,6]

In this work, a 5-stage IC detector design with enhanced electron barriers[4,5] is adopted. The samples are grown on Zn-doped 2 in. (001) GaSb substrates with a solid-source molecular beam epitaxy (MBE) system. The absorber is composed of 30-periods (∼140 nm) of non-intentionally doped InAs/GaSb (18 Å/27 Å) T2-SL, the eR region is consist of InAs/Al(In)Sb coupled MQWs, and the eT region is consist of 4–6 pairs of GaSb/AlSb MQWs. The samples are first processed into single pixel devices to evaluate the detector performance. Despite the relatively thin absorber, these MWIR single-pixel IC detectors are operational up to 450 K under zero-bias, as shown in Fig. 2. Note that no special noise suppression technique is adopted; the signal from the IC detector is directly fed into a current pre-amplifier and subsequently into the spectrometer. The record high operating temperature of the IC detectors demonstrates the great potential of these structures for HOT applications. The 50% cutoff wavelength is ∼4.4 μm at 300 K. The dark current of the single pixel devices is as low as 1.10×10^{-7} A/cm^2 at −5 mV and 150 K. Further details about the single-pixel IC device results can be found in Ref. 5.

These wafers are then processed into 320 × 256 FPA, with pixel size of 24 × 24 μm^2 and pitch of 30 μm (filling factor 64%). The mesa is fabricated by contact photolithography and BCl_3-based inductance coupled plasma etching. A 250-nm-thick Si_3N_4 film is then deposited for passivation and electrical isolation. Following the formation of Ohmic contacts, under-bump metallization and Indium bumps are deposited. The diced FPAs are then hybridized to Indigo

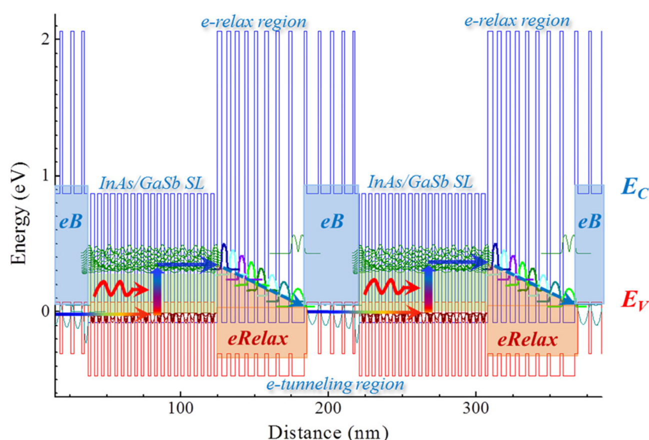

FIG. 1. Band structure diagram of (two stages in) an interband cascade photodetector. The transport of carriers is shown by arrows. The incoming photons are absorbed in the InAs/GaSb T2-SL absorbers, generating electron-hole pairs. The electrons will diffuse into the electron relaxation region, and then effectively transport into the valence band of the next stage, through fast LO-phonon assisted intraband relaxation and interband tunneling.

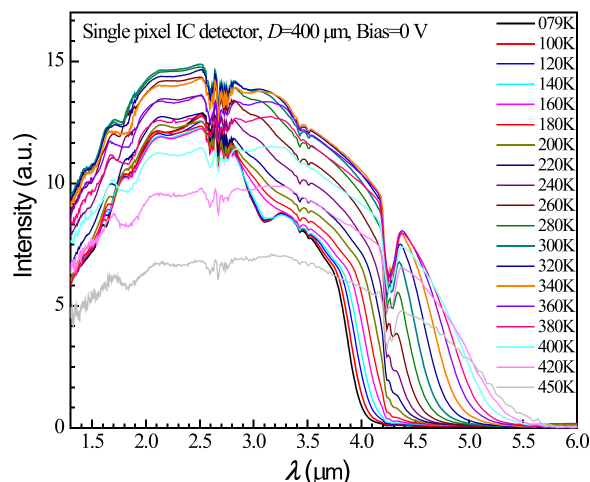

FIG. 2. Response spectra of MWIR IC single-pixel detectors, the device is operational up to 450 K under zero-bias.

ISC9705 read-out integrated circuits (ROIC) using a Suss Microtech FC150 flip-chip bonder. After hybridization, the substrate is thinned down using a Logitech PM5 polishing system. In this work, the *p*-GaSb substrate is not fully removed due to the lack of proper etch stop layers. The FPAs are mounted and wire-bonded onto ceramic leadless chip-carriers, and are then characterized by using a SE-IR CIR-HD infrared camera characterization system equipped with F = 2.3 optics (field-of-view 24.5 degrees) and a Sterling cooler. Radiometric measurements are performed with a calibrated Mikron M315 black-body placed 40 cm away from the FPAs.

Figure 3 shows the IR images acquired from IC FPAs at 80 K. A two-point non-uniformity correction (NUC, between 25 °C and 32 °C) is used to remove non-uniformity and fixed pattern noise between pixels and read-out circuit, prior to image acquisition. Figure 3(a) is an IR image acquired from the first IC FPA with ∼40 μm of *p*-GaSb substrate (denoted as FPA-1 hereafter). The horizontal lines in the thermal image are due to the noise imposed by vibrations from the Sterling cooler. Since the *p*-type GaSb substrate is highly absorbent to the incoming IR photons, it will significantly reduce the overall SNR and thus the attainable NEDT. Fig. 3(b) shows IR images acquired from an IC FPA with the

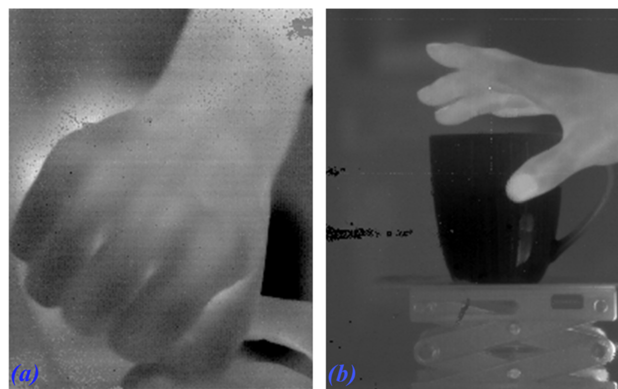

FIG. 3. Infrared images acquired from IC FPAs operated at 80 K. A simple two-point NUC was used. Brighter areas indicate warmer regions. (a) is acquired from an IC FPA with 40 μm p-GaSb substrate; (b) is taken from an IC FPA with ∼10 μm *p*-GaSb substrate.

This article is copyrighted as indicated in the article. Reuse of AIP content is subject to the terms at: http://scitation.aip.org/termsconditions. Downloaded to IP: 68.35.133.217 On: Thu, 07 Aug 2014 16:31:46

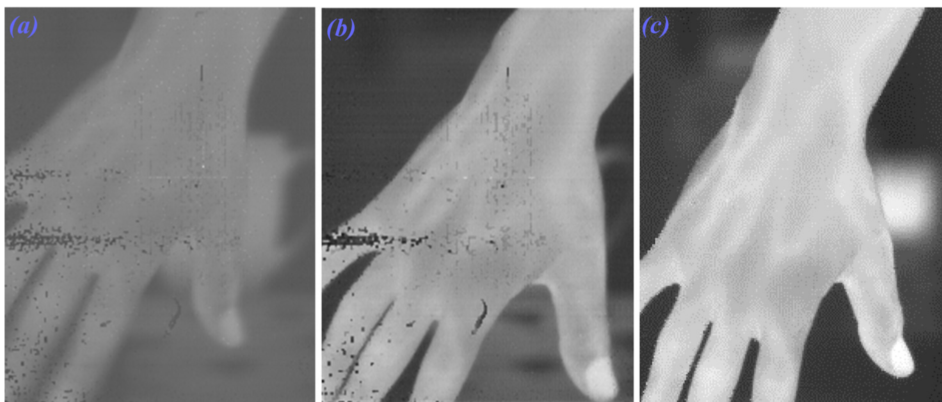

FIG. 4. Thermal images acquired from IC FPA-2 at 80 K with integration time of 5, 15, and 30 ms, respectively. A simple two-point NUC was used in (a) and (b), and a dead-pixel removal process was adopted in (c) in addition to the NUC.

GaSb substrate etched down to ∼10 μm (denoted as FPA-2). The thermal image quality is significantly better than that shown in Fig. 3(a). In the thermal image of Fig. 3(b), the cup is filled with cold water, and the temperature gradient on the cup handle is clearly seen, showing good temperature resolution even under low irradiance conditions. The blood vein is clearly distinguishable from the normal skin in Fig. 3(b), which demonstrates very good temporal and spatial resolution of the IC IR imagers.

It is worth noting that the IC FPAs have only a total T2-SL absorber thickness of 0.7 μm, which corresponds to an absorption quantum efficiency (QE) of approximately 28% in a double-pass scheme, as determined from carefully designed absorption measurements. By taking the surface reflectance (between air and GaSb, estimated from refractive index measured with IR variable angle Ellipsometry) and free carrier absorption in the *p*-GaSb substrate (the absorption coefficient is extracted from optical transmission measurement) into consideration, the absorption QE of IC FPA-1 is ∼12.4%, whereas the absorption QE of IC FPA-2, which has a 10-μm-substrate is ∼16.4%. These numbers could be somewhat overestimated, as the incoming photon losses associated with Ge window, MWIR band pass filter, and IR lens are neglected. Since the external QE of IC detectors equals to absorption QE divided by the number of stages, which means the external QE of the IC FPAs is as low as ∼3.1%. It should be noted that the low QE is not a fundamental limitation to IC devices and FPAs. The performance of IC FPAs can be significantly improved by adopting thicker InAs/GaSb SL absorbers and full removing the GaSb substrate. With the relatively low QE and much lower noise, IC FPAs are expected to have a wider dynamic range. As the integration capacitor will not be easily saturated, even with lower frame rates and higher irradiance. In fact, our measurement suggests that the IC FPAs are operational with irradiance (between 3–5 μm) up to 1.2×10^{17} ph/cm^2 s, even under the longest integration time of 33.2 ms for our test system.

To investigate how IC detectors with relatively low QE and high SNR work with standard read-out technology (designed for high QE detectors), the IC FPAs are tested with different integration times. Figure 4 shows IR images acquired from IC FPA-2 at 80 K with an integration time of 5, 15, and 30 ms, respectively. In Figs. 4(a) and 4(b), only a simple two-point NUC is applied. In Fig. 4(c), a dead-pixel removal process is adopted in addition to the NUC. Despite the 3% external QE, the blood vein in the image can still be clearly distinguished from normal skin, even with a 5 ms integration time. This is partially attributed to the higher impedance in IC detectors, which can greatly enhance the injection coupling efficiency of photo-carriers into the integration capacitor of the ROIC, particularly in HOT applications. Fig. 4 shows that the thermal image quality improves steadily as the integration time increases, and the images show no sign of saturation. Higher image quality under longer integration time is associated with the relatively low QE, which is not fundamental to IC detectors as stated earlier. In fact, IC detectors might have higher speed than conventional IR photodetectors, as the photo-generated electrons in IC detector travel through a significantly shorter distance for collection. Thus, much higher frame rates could be expected with optimized IC detector design and/or customized read-out technologies.

IC FPA-2 is operational up to 180 K, with clearly distinguishable human facial features at above 170 K, showing the potential in IC devices for HOT operations. An IR image acquired from IC FPA-2 at 170 K is shown in the inset of Fig. 5. The relatively large discrepancy of the highest operation temperature between the IC FPA and single-pixel device is believed to be related to multiple possible technological factors, including pronounced surface leakage, mismatched read-out technology, non-uniformity in our material growth

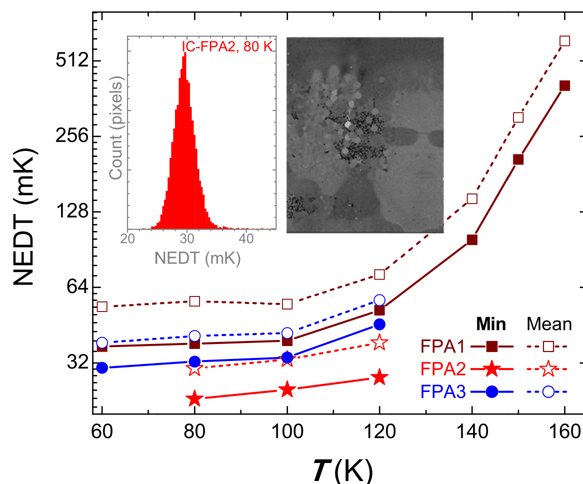

FIG. 5. Minimum (bold lines, the mean NEDT value among the top 1% pixels) and mean (dotted lines) NEDT of three IC FPAs at various operation temperatures. The insets are the NEDT histogram for 96 × 85 pixels in a selected area of IC FPA-2 at 80 K, and an IR image acquired from IC FPA-2 at 170 K, respectively.

This article is copyrighted as indicated in the article. Reuse of AIP content is subject to the terms at: http://scitation.aip.org/termsconditions. Downloaded to IP: 68.35.133.217 On: Thu, 07 Aug 2014 16:31:46

and fabrication process, and mechanical vibrations in the characterization setup originated from the Sterling cooler.

Radiometric measurements under various operation conditions, including different operation temperatures, bias voltages, and illumination intensities, were performed with these IC FPAs. The NEDT was measured by acquiring a sequence of 100 image scans with the IC focal plane arrays exposed to a blackbody with varied temperatures. NEDT is then determined by the blackbody temperature difference divided by the SNR, where the noise is computed from the standard deviation of each individual pixel over the 100 frames. In our NEDT calculations, a selected square area with less defective pixels (with about 1/4 of the 320×256 pixels) is used. Fig. 5 shows the extracted NEDT (for $T_2 = 80\,°C$, $T_1 = 25\,°C$) as a function of operation temperatures for three IC FPAs tested. The inset is the NEDT histogram of 8100 pixels from a selected square area in IC FPA-2 operated at 80 K. The operation bias, black-body radiation intensity was kept constant during the measurement for each FPA. The optimum operation bias is temperature dependent. Therefore, the NEDT could be further improved by optimizing the FPA settings at each individual operation temperatures. Despite the low QE associated with the thin absorbers and the absorbent *p*-GaSb substrate, the minimum NEDT (taken from top 1% pixels from a selected area in the 320×256 IC FPA, with over 8000 pixels) and mean NEDT for IC FPA-2 are 24 mK and 30 mK at 80 K, respectively. The mean and minimum NEDT are almost constant up to 120 K. The sharp increase in NEDT at above 120 K is still not well understood; we speculate that it could be associated with the surface leakage due to un-optimized passivation and/or relatively high shot noise due to the moderate operation bias at HOTs. Further improvements can be expected by optimizing the FPA fabrication, refining the IC detector design such as adopting a thicker absorber.

Even though the IC detector is photovoltaic in nature, with best SNR expected at zero-bias,[5] a moderate "turn-on" bias of around 0.3 V is required for higher image quality in our IC FPAs. Aside from an operation bias required to remove spatial non-uniformities between the read-out units and the IC pixels, the major reasons could include the relatively low QE in our IC devices[5] and the noise components contributed from the read-out circuit. Because of the very low noise characteristics in IC detectors,[5–7] the overall noise could be limited by the read-out circuit, even under higher operation bias. Therefore, the image quality of our IC FPAs could be more related to the signal intensity. As indicated by our bias dependent QE measurements on single-pixel devices, the zero-bias responsivity is about $0.55 \times \eta_{sat}$, and increases to $\sim 0.90 \times \eta_{sat}$ at 0.56 V, where η_{sat} is the saturated quantum efficiency obtained under sufficient operation bias. Thus, optimum image quality is obtained with certain turn-on operating bias. It should be clarified that the turn-on bias in our IC detectors is associated with our device design, and is not a fundamental limit to the performance of IC detectors and FPAs. As demonstrated in some of the prior works,[5,6] IC devices are operational under zero-bias with an optical response of over 90% of the saturation value.

To validate our speculations, radiometric measurements were performed on IC FPAs under different irradiances and operation biases. Figure 6 shows the mean NEDT trend of IC FPA-2 with respect to irradiance and detector bias at both 100 and 120 K. As seen from Fig. 6, the mean NEDT decreases with increased irradiance. Our analysis on FPA noise characteristics show that the FPA noise initially decreases as the irradiance increases, and then remains almost constant under medium through high irradiance conditions. This indicates that the IC FPA is likely not limited by the signal noise. One interesting observation from Fig. 6(a) is that, at lower operating temperatures, the optimum operation bias for the IC FPA is dependent on irradiance intensity, while under higher irradiance, an improved NEDT is obtained at higher operation bias. This could be attributed to different dominating noise mechanisms in the IC FPAs at lower temperatures. Since the signal is relatively small under lower irradiance conditions, the noise could be mainly contributed from ROIC or shot noise in detector pixels, and therefore, a higher SNR is obtained under lower operation biases. As the operation temperature increases, the optimum operation bias is reduced, as shown in Fig. 6(b). This could be associated with the increased contribution of noise from the IC detector pixels. Since the dark current in IC detectors scales with applied bias voltage, an increased bias could significantly increase the dark current and thereby reduce the SNR.

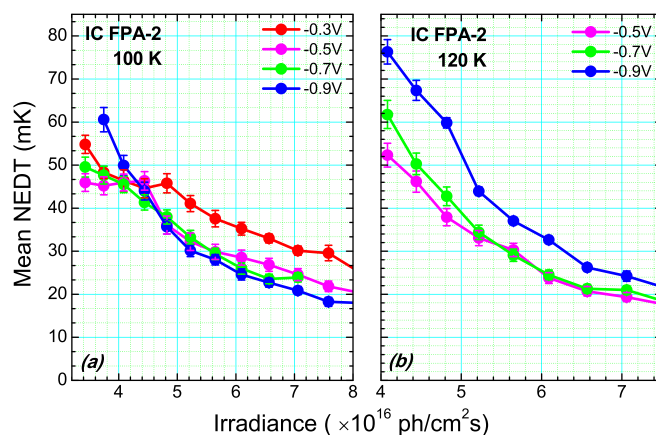

FIG. 6. Mean NEDT of IC FPA-2 under various irradiance and bias conditions at (a) 100 K and (b) 120 K. The operation bias of the detector pixels is estimated from the overall operation bias on the ROIC and detector pixels, so some uncertainty may exist.

In conclusion, MWIR FPAs based on interband cascade photodetectors with a multi-junction/stage design, is demonstrated. The single-pixel MWIR IC devices show very low dark current, and are operational up to 450 K. Despite of the un-optimized device design and FPA fabrication, as well as mis-matched ROIC, the IC FPAs demonstrate good temperature performance. The IC FPA is operational up to 180 K, with a minimum NEDT of 24 mK obtained at 80 K. It is believed that the efficient photo-carrier extraction and low-noise features offer IC detectors great potential as high performance IR imagers, particularly for high operating temperature applications.

This work was supported in part by AFRL under Grant No. FA9453-13-1-0284. Other US government funding agencies are also acknowledged. The single-pixel device

This article is copyrighted as indicated in the article. Reuse of AIP content is subject to the terms at: http://scitation.aip.org/termsconditions. Downloaded to IP: 68.35.133.217 On: Thu, 07 Aug 2014 16:31:46

processing was performed at the Center for Integrated Nanotechnologies, a US Department of Energy, Office of Basic Energy Sciences user facility at Sandia National Laboratories, for which we would like to thank John Nogan for the technical assistance.

[1]L. Zheng, M. Tidrow, S. Bandara, L. Aitcheson, and T. Shih, Proc. SPIE **8012**, 80120S (2011).
[2]R. Rehm, M. Walther, J. Schmitz, J. Fleißner, F. Fuchs, J. Ziegler, and W. Cabanski, Opto-Electron. Rev. **14**, 19 (2006).
[3]S. A. Pour, E. K. Huang, G. Chen, A. Haddadi, B.-M. Nguyen, and M. Razeghi, Appl. Phys. Lett. **98**, 143501 (2011).
[4]A. Haddadi, S. Ramezani-Darvish, G. Chen, A. M. Hoang, B.-M. Nguyen, and M. Razeghi, J. Quantum Electron. **48**, 221 (2012).
[5]Z.-B. Tian, T. Schuler-Sandy, and S. Krishna, Appl. Phys. Lett. **103**, 083501 (2013), and references therein.
[6]Z. Tian, R. T. Hinkey, R. Q. Yang, Y. Qiu, D. Lubyshev, J. M. Fastenau, A. W. K. Liu, and M. B. Johnson, J. Appl. Phys. **111**, 024510 (2012).
[7]R. Q. Yang, Z. Tian, J. F. Klem, T. D. Mishima, M. B. Santos, and M. B. Johnson, Appl. Phys. Lett. **96**, 063504 (2010).
[8]J. Piotrowski, P. Brzozowski, and K. Jozwikowski, J. Electron. Mater. **32**, 672 (2003).

This article is copyrighted as indicated in the article. Reuse of AIP content is subject to the terms at: http://scitation.aip.org/termsconditions. Downloaded to IP: 68.35.133.217 On: Thu, 07 Aug 2014 16:31:46